General Disclaimer

One or more of the Following Statements may affect this Document

- This document has been reproduced from the best copy furnished by the organizational source. It is being released in the interest of making available as much information as possible.

- This document may contain data, which exceeds the sheet parameters. It was furnished in this condition by the organizational source and is the best copy available.

- This document may contain tone-on-tone or color graphs, charts and/or pictures, which have been reproduced in black and white.

- This document is paginated as submitted by the original source.

- Portions of this document are not fully legible due to the historical nature of some of the material. However, it is the best reproduction available from the original submission.

NASA TECHNICAL MEMORANDUM

NASA TM X-71801

NASA TM X-71801

CHARGE EXCHANGE IN ZINC-NEON

by Donald L. Chubb
Lewis Research Center
Cleveland, Ohio 44135

TECHNICAL PAPER to be presented at
Twenty-eight Annual Gaseous Electronics Conference
sponsored by the American Physical Society
Rolla, Missouri, October 21-24, 1975

CHARGE EXCHANGE IN ZINC-NEON

by Donald L. Chubb
Lewis Research Center

ABSTRACT

Excitation of the 4d and 5p levels of Zn^+ by charge exchange between Ne^+ and Zn was investigated. From measured electron temperature and line intensity ratios it was concluded that charge exchange is the dominate mechanism for populating the $4d^2D_{5/2}$ level of Zn^+. Comparison of Zn-Ne and Zn-Ar results imply the same conclusion. No evidence for charge exchange as the dominant pumping mechanism for the $5p^2P_{1/2}$, $5p^2P_{3/2}$, or $4d^2D_{3/2}$ levels was obtained.

INTRODUCTION

In investigating lasing in He-Ne-Zn, Collins[1] observed evidence for charge exchange between Ne^+ and Zn atoms to produce excited Zn^+ ions. The observed reaction was the following.

$$Ne^+ + Zn \rightarrow Ne + Zn^+(4d^2D_{5/2} \text{ or } 4d^2D_{3/2}) + \Delta E \qquad (1)$$

where $\Delta E = I_{Ne} - (I_{Zn} + E_{Zn^+})$ is the energy defect, I is the ionization potential and E is the excitation potential. For Zn^+ $(4d^2D_{3/2})$, $\Delta E = 0.155$ eV and for $Zn^+(4d^2D_{5/2})$ $\Delta E = 0.149$ eV.

If the cross section for the reaction described by Equation (1) is large enough, it may be possible to selectively populate the 4d levels in Zn^+. In this case lasing may occur at wavelengths of 2064 Å, 2102 Å, or 2100 Å for $4d \rightarrow 4p$ transitions. As a result, an experimental investigation of the Zn-Ne system was undertaken. The experiment was similar to one used to study charge exchange in Ca-Xe[2]. A steady-state flowing Ne plasma was produced in a low power (500 W) arc source. Zinc was injected into the plasma beam where charge exchange occurs between Ne^+ and Zn. From relative intensity and electron temperature measurements it is possible to determine if charge exchange or electron collisional excitation is responsible for populating a particular level of Zn^+.

In addition to charge exchange to the 4d levels of Zn^+, there is also the possibility of charge exchange to the 5p levels since ΔE is small.

$$Ne^+ + Zn \rightarrow Ne + Zn^+(5p^2P_{1/2} \text{ or } 5p^2P_{3/2}) + \Delta E \qquad (2)$$

For the $5p^2P_{1/2}$ level, $\Delta E = -0.397$ eV and for the $5p^2P_{3/2}$ level, $\Delta E = -0.426$ eV. In analyzing the experimental data charge exchange to

E-8481

both the 4d and 5p levels will be considered.

ANALYSIS

By relating the measured intensity ratios to the power input to the plasma source, it is possible to deduce whether charge exchange or electron collisions are responsible for populating a particular level. The intensity ratios are related to the electron temperature through the use of the continuity equations for the various levels. Also, the electron temperature was measured as a function of power input. As a result, a relation between intensity ratios and power input is obtained.

Figure 1 shows an energy level diagram for the zinc ion. Also shown are the relevant wavelengths λ_{ij} and transition probabilities A_{ij}. The transition probabilities were calculated using the Bates-Damgaard[3] technique at Colorado State University.[4] The solid lines indicate the transitions where intensity measurements were made in this experiment. It was not possible to measure the 5p → 5s transition intensities because the monochromator used had a wavelength limitation of 7000 Å.

The continuity equation under steady-state conditions[2] for the i^{th} level in Figure 1 states that the sum of the net collisional pumping rate, W_i, and spontaneous decay rate into the i^{th} level from levels above the i^{th} is equal to the spontaneous decay rate from the i^{th} level.

$$W_i + \sum_{j=i+1}^{8} n_j A_{ji} = n_i \sum_{j=1}^{i-1} A_{ij} \tag{3}$$

The number density of the i^{th} level is denoted by n_i. The collisional pumping rate, W_i, includes both electron excitation and charge transfer collisions. All cascading from levels above the 5p has obviously been neglected. Charge exchange pumping is not expected for levels above the 5p. As a result, any contributions to Equation (3) resulting from cascading will be independent of charge exchange. Therefore, all charge exchange contributions to the population of the 5p or 4d levels are included in Equation (3).

Using Equation (3) for the eight levels in Figure 1 the measured intensity ratios can be related to the pumping rates of these levels. An intensity ratio is related to the level number densities by the following relation.

$$R_{\lambda_{ij}}^{\lambda_{pq}} = \frac{\lambda_{ij} A_{pq}}{\lambda_{pq} A_{ij}} \left(\frac{n_p}{n_i}\right) \tag{4}$$

Therefore, applying Equation (3) to the eight levels in Figure 1 yields the following results.

$$R_{2025}^{2100} = \frac{2025}{2100} \frac{W_6}{W_3 + \frac{A_{43}}{A_{42} + A_{43}} W_u + \frac{A_{53}}{A_{52} + A_{53}} W_5 + W_6} \tag{5}$$

$$R_{2062}^{2064} = \frac{2062}{2064} \frac{W_5}{W_2 + \frac{A_{42}}{A_{42} + A_{43}} W_u + \frac{A_{52}}{A_{52} + A_{53}} W_5} \tag{6}$$

$$R_{2062}^{2502} = \frac{2062}{2502} \frac{A_{42}}{A_{42} + A_{43}} \frac{W_u}{W_2 + \frac{A_{42}}{A_{42} + A_{43}} W_u + \frac{A_{52}}{A_{52} + A_{53}} W_5} \tag{7}$$

$$R_{2025}^{2558} = \frac{2025}{2558} \frac{A_{43}}{A_{42} + A_{43}} \frac{W_u}{W_3 + \frac{A_{43}}{A_{42} + A_{43}} W_u + \frac{A_{53}}{A_{52} + A_{53}} W_5 + W_6} \tag{8}$$

$$R_{2558}^{2100} = \frac{2558}{2100} \frac{A_{42} + A_{43}}{A_{43}} \frac{W_6}{W_u} \tag{9}$$

$$R_{2558}^{2064} = \frac{2558}{2064} \frac{A_{52}}{A_{43}} \left(\frac{A_{42} + A_{43}}{A_{52} + A_{53}} \right) \frac{W_5}{W_u} \tag{10}$$

where

$$W_u = W_4 + W_7 + W_8 \tag{11}$$

In obtaining Equations (5) to (10) the approximations $A_{74} >> A_{75}, A_{71}$ and $A_{84} >> A_{85}, A_{86}, A_{81}$ have been made.

To relate the intensity ratios to the electron temperature, the pumping rates, W_i, must be expressed in terms of the plasma properties. It is assumed that electron collisions and charge exchange with Ne^+ can pump the 4d and 5p levels. However, only electron collisions are assumed to pump the 5s and 4p levels.

Electron collisions between any of the many Zn and Zn^+ levels can produce Zn^+ in the eight levels shown in Figure 1. However, because of the large energy difference between Zn atom states and these Zn^+ states, we neglect electron pumping of these levels resulting from electron-Zn atom collisions. Therefore, the only electron pumping to be considered

will be excitation from low energy Zn^+ states to higher energy Zn^+ excited states. As a result, the electron pumping rate for any of the excited Zn^+ levels is the following.

$$(W_j)_e = n_e \sum_{i=1}^{j-1} n_i S_{ij}(T_e) \tag{12}$$

The term S_{ij}, which is a function of the electron temperature, T_e, is the collisional rate coefficient (m^3/sec) for excitation of the jth level resulting from electron-ith level Zn^+ collisions.

$$S_{ij} \equiv \langle (\sigma_{ij})_e v_e \rangle \tag{13}$$

where $(\sigma_{ij})_e$ is the electron excitation cross section for $i \rightarrow j$ transitions, v_e is the electron velocity, and $\langle\ \rangle$ denotes an average over the electron distribution function.

For analyzing the experimental data it is only necessary to know whether S_{ij} is an increasing or decreasing function of electron temperature. Therefore, consider two functional forms for σ_{ij} that should be reasonable approximations for Zn^+. First of all, it has been suggested[5] that $(\sigma_{ij})_e \sim 1/v_e^2$. In this case for a Maxwellian electron distribution S_{ij} is the following.

$$S_{ij} = C_{ij}\left(\frac{1}{kT_e}\right)^{1/2} \exp\left(-\frac{E_{ij}}{kT_e}\right) \qquad (\sigma_{ij})_e \sim \frac{1}{v_e^2} \tag{14a}$$

where $E_{ij} = E_j - E_i$ is the energy difference between the j and i levels, k is the Boltzmann constant. The electron excitation rate coefficient given by Equation (14a) increases with T_e until $kT_e = 2E_{ij}$ and then decreases for $kT_e > 2E_{ij}$. The constant C_{ij} has two different forms depending on whether the transition is allowed or forbidden. Recent experimental results[6] for $4s \rightarrow 4p$ electron excitation in Ca^+ suggest that $(\sigma_{ij})_e$ = constant is a good approximation for low electron energies. In this case for a Maxwellian electron distribution S_{ij} is the following.

$$S_{ij} = K_{ij}\sqrt{kT_e}\left(\frac{E_{ij}}{kT_e} + 1\right) \exp\left(-\frac{E_{ij}}{kT_e}\right) \qquad (\sigma_{ij})_e = \text{constant} \tag{14b}$$

This is a monotonically increasing function of T_e.

In this experiment $kT_e < 2E_{ij}$ for the $i \rightarrow j$ transitions of interest (denoted by solid lines in Fig. 1). Therefore, assuming that reasonable approximations for S_{ij} are given by either Equations (14a) or (15b), then it can be concluded that S_{ij} will be an increasing

function of T_e for the transitions denoted by solid lines in Figure 1.

For the case of charge exchange, only collisions between Ne^+ and Zn ground state atoms need be considered. Therefore, the charge exchange pumping rate to the ith level is the following:

$$(W_j)_c = n_o n_{Ne^+} L_{oj} \tag{15}$$

where n_o is the number density of ground state Zn atoms, n_{Ne^+} is the number density of Ne^+ and L_{oj} is the collisional rate coefficient (m^3/sec) for charge exchange excitation of the jth level resulting from Zn-Ne^+ collisions. In this experiment the relative velocity U between Ne^+ and Zn, is much greater than the ion thermal speed. Also, assuming the charge exchange cross section, σ_{oj}, is nearly independent of U the charge exchange rate coefficient can be approximated as follows.

$$L_{oj} = U\sigma_{oj} \tag{16}$$

Equation (16) shows that the charge exchange rate coefficient is independent of T_e.

Using Equations (12), (15), and (16) the intensity ratios can now be written in terms of the plasma parameters. For comparison with the experimental data, two limiting forms of the intensity ratios are necessary. First, when electron pumping of the 5s, 4d, and 5p levels of Zn^+ is negligible. Second, when change exchange pumping of the 5s, 4d, and 5p levels is negligible. When electron pumping is negligible

$$(W_u)_c = n_o n_{Ne^+} U(\sigma_{07} + \sigma_{08}) \tag{17a}$$

$$(W_5)_c = n_o n_{Ne^+} U\sigma_{05} \tag{17b}$$

$$(W_6)_c = n_o n_{Ne^+} U\sigma_{06} \tag{17c}$$

And since only electron collisions can pump the 4p levels,

$$W_2 = n_e n_1 S_{12} \tag{17d}$$

$$W_3 = n_e n_1 S_{13} \tag{17e}$$

Since levels 2 and 3 have nearly the same energy, they should be close to being in equilibrium. Therefore, deexcitation (3 → 2) should nearly balance excitation (2 → 3). As a result, an S_{23} term in Equation (17e) has been neglected.

Substituting Equations (17) in Equation (5) yields the following result for the T_e dependence when charge exchange predominates over electron pumping of the 5s, 4d, and 5p levels.

$$\left(R_{2025}^{2100}\right)_c \sim (NS_{13} + K)^{-1} \tag{18}$$

where

$$N = \frac{n_e n_1}{n_o n_{Ne^+}} \tag{19}$$

$$K = U\left[\frac{A_{43}}{A_{42} + A_{43}} (\sigma_{07} + \sigma_{08}) + \frac{A_{53}}{A_{52} + A_{53}} \sigma_{05} + \sigma_{06}\right] \tag{20}$$

Consider how the term N given by Equation (19) depends on the electron temperature. As the electron temperature increases, more ionization of Zn and Ne will occur. Therefore, in order to maintain charge neutrality ($n_e \approx n_1 + n_{Ne^+}$), n_e, n_1, and n_{Ne^+} will all be increasing functions of T_e, while n_o will decrease with increasing T_e. Also, in order to satisfy $n_e \approx n_1 + n_{Ne^+}$ the mean ion density, n_{Ne^+} cannot increase faster than n_e. Therefore, the term N will be an increasing function of T_e. As has already been pointed out, S_{13} is an increasing function of T_e for this experiment. As a result, the intensity ratio R_{2025}^{2100} will be a decreasing function of T_e if charge exchange is much greater than electron pumping of the 5s, 4d, and 5p levels of Zn^+. The same conclusion applies to the R_{2062}^{2064}, R_{2062}^{2502}, and R_{2025}^{2558} intensity ratios.

Now consider the intensity ratios R_{2558}^{2100} and R_{2558}^{2064}. For charge exchange pumping of the 4d and 5p levels, Equations (9) and (10) yield the following.

$$\left(R_{2558}^{2100}\right)_c = \frac{2558}{2100} \frac{A_{42} + A_{43}}{A_{43}} \left(\frac{\sigma_{06}}{\sigma_{07} + \sigma_{08}}\right) \tag{21}$$

$$\left(R_{2558}^{2064}\right)_c = \frac{2558}{2064} \frac{A_{52}}{A_{43}} \left(\frac{A_{42} + A_{43}}{A_{52} + A_{53}}\right)\left(\frac{\sigma_{05}}{\sigma_{07} + \sigma_{08}}\right) \tag{22}$$

Equations (21) and (22) show that R_{2558}^{2100} and R_{2558}^{2064} will be independent of the electron temperature if charge exchange is the dominant pumping mechanism.

Now consider the situation when only electron collisions are responsible for populating all the Zn^+ levels. For this experiment $kT_e \approx 10$ eV. Therefore, it is expected that the 4s and 4p levels of Zn^+ will be highly populated. As a result, there will be significant electron collisional excitation from the 4p levels to the 5s and 4d levels. However, since the energy of the 5p levels is greater than the energies of the 5s and 4d levels and also since $5p \rightarrow 4p$ is a forbidden transition the densities of the 5p levels should be negligible. As a result, the 5p levels are neglected in Equation (3) for the case of electron

pumping only. Also, since the $4p^2P_{1/2}$ and $4p^2P_{3/2}$ levels are very close in energy, $E_{23} = 0.1$ eV, they should be close to being in equilibrium. Therefore,

$$\frac{n_3}{n_2} = \frac{g_3}{g_2} \exp\left(-\frac{E_{23}}{kT_e}\right) \approx \frac{g_3}{g_2} = 2 \tag{23}$$

where g denotes the degeneracy of a level. Experimental results indicate that n_3/n_2 is independent of T_e. This will be discussed further in the EXPERIMENTAL RESULTS section. Since the energy difference (~11 eV) between the 4s and 5s levels and the 4s and 4d (~12 eV) is large, as well as the transitions $5s \rightarrow 4s$ and $4d \rightarrow 4s$ being forbidden, it is reasonable to assume $S_{14} = S_{15} = S_{16} = 0$.

Under the above assumptions, Equation (3) for the $4d^2D_{5/2}$ level ($i = 6$) and Equation (4) yield the following.

$$\left(R_{2025}^{2100}\right)_e = \frac{2025}{2100} \frac{1}{A_{31}} \left(\frac{n_2}{n_3} S_{26} + S_{36}\right) n_e \tag{24}$$

It has already been pointed out that all the electron excitation rate coefficients, S_{ij}, will be increasing functions of T_e. Also, n_e will increase with increasing T_e. Therefore, with the assumption that $n_2/n_3 =$ constant, Equation (24) shows that R_{2025}^{2100} will be an increasing function of T_e if electron collisions are the dominant pumping mechanism of all the levels. This same conclusion applies to R_{2062}^{2064}, R_{2062}^{2502}, and R_{2025}^{2558}.

Again, under the above assumptions, Equation (3) for the $4d^2D_{5/2}$ level ($i = 6$) and the $5s^2S_{1/2}$ ($i = 4$) level together with Equation (4) yield the following.

$$\left(R_{2558}^{2100}\right)_e = \frac{2558}{2100} \frac{A_{42} + A_{43}}{A_{43}} \left(\frac{\frac{n_2}{n_3} S_{26} + S_{36}}{\frac{n_2}{n_3} S_{24} + S_{34}}\right) \tag{25}$$

Assume that $E_{26} \approx E_{36}$ and $E_{24} \approx E_{34}$. Then if all the electron excitation rate coefficients in Equation (25) behaved according to Equations (14a) or (14b), $(R_{2558}^{2100})_e$ would be an increasing function of T_e. However, since it is not clear that all S_{ij} have the same T_e dependence, it is not possible to conclusively state whether $(R_{2558}^{2100})_e$ should be an increasing or decreasing function of T_e. The same conclusion applies to $(R_{2558}^{2064})_e$.

Now consider the situation when charge exchange populates the $4d^2D_{5/2}$ level but electron collisions populate the other levels. The

T_e dependence of R_{2025}^{2100} will be the same as that in Equation (18) ($\sigma_{05} = \sigma_{07} = \sigma_{08} = 0$ in Eq. (20) and assuming $W_6 >> W_u, W_5$). Therefore, if charge exchange is the mechanism for populating the $4d^2D_{5/2}$ level, the R_{2025}^{2100} intensity ratio will decrease with increasing T_e. The result for R_{2558}^{2100} is obtained by substituting $W_u = n_e[n_2 S_{24} + n_3 S_{34}]$ and Equation (17c) in Equation (9),

$$\left(R_{2558}^{2100}\right)_{e-c} \sim \left[N'\left(S_{24} + \frac{n_3}{n_2} S_{34}\right)\right]^{-1} \tag{26}$$

where

$$N' = \frac{n_e n_2}{n_o n_{Ne^+}} \tag{27}$$

Similar to N the quantity, N' will be an increasing function of T_e. Also, S_{24} and S_{34} are increasing functions of T_e. Therefore, since $n_3/n_2 \approx$ constant Equation (26) shows that R_{2558}^{2100} will decrease with increasing T_e if the $4d^2D_{5/2}$ level is pumped by charge exchange and all the other levels by electron collisions.

EXPERIMENTAL RESULTS

Zn-Ne Results

The experimental apparatus used for this experiment is described in Reference 2. A steady-state flowing neon plasma is produced in a low power arc source. The velocity of the flow is the order of 10^6 cm/sec. Zinc is injected into the flow by sublimation from a zinc ribbon. The zinc ribbon was wrapped around a nichrome wire which was resistively heated to zinc sublimation temperatures. Varying the amount of zinc injection had negligible effect on the intensity ratios to be discussed below.

Electron temperatures were measured with a double Langmuir probe. The double probe cannot be used in a plasma that is seeded with a metal. In such a situation the probe becomes contaminated with the metal so that reliable probe current versus probe voltage data cannot be obtained. Therefore, probe data was taken only in pure neon.

Relative intensity measurements were made with a 1/2-m focal length scanning monochromator. The monochromator viewed the plasma through a quartz window in the region where zinc was injected. In the wavelength region (2000 Å - 2600 Å) where the intensity measurements were made, the monochromator transmission changes rapidly with wavelength. As a result, it was not possible to obtain an accurate calibration of the monochromator. In presenting the intensity ratio data, therefore, the intensity ratios have been normalized. Normalization will remove the monochromator

transmission from the results. The maximum intensity ratio was chosen as the normalization factor. Normalized intensity ratios will be denoted as $\bar{R}$.

In the ANALYSIS section the approximation n_3/n_2 = constant was used. From the measured intensity ratio $(R^{2025}_{2062})_m = n_3/n_2$ it is possible to evaluate this approximation. The measured intensity ratio, $(R^{2025}_{2062})_m$, is related to the actual intensity ratio as follows.

$$\left(R^{2025}_{2062}\right)_m = \frac{T_{2025}}{T_{2062}} R^{2025}_{2062} = \frac{2062}{2025} \frac{T_{2025}}{T_{2062}} \frac{A_{31}}{A_{21}} \frac{n_3}{n_2} \tag{28}$$

where T_λ is the transmission of the optics (window, monochromator, and PM tube) at wavelength λ. As mentioned above, it was not possible to get an accurate measurement of T_λ. However, for the Zn-Ne data reported here $(R^{2025}_{2062})_m$ varied from 1.27 to 1.39. Since this is less than a 10 percent variation, the approximation n_3/n_2 = constant appears to be valid.

Figure 2 shows $\bar{R}^{2100}_{2025}$ and $\bar{R}^{2064}_{2062}$ as functions of the input power to the plasma source. Also shown is the electron temperature in pure Ne. With the addition of Zn the magnitude of T_e should be reduced but not the shape of the T_e versus power input curve. For input power, P_i, below 280 watts, the electron temperature behavior is erratic. However, for $280 \leq P_i \leq 460$ watts the electron temperature is an increasing function of P_i.

For $280 \leq P_i \leq 460$ watts the intensity ratio $\bar{R}^{2100}_{2025}$ decreases. As discussed earlier, this is the electron temperature dependence expected if charge exchange is the predominate pumping mechanism of the 4d and 5p levels (see Eq. (18)). However, $\bar{R}^{2064}_{2062}$ increases with increasing T_e. This is the T_e dependence expected if all the levels are pumped by electron collisions (see Eq. (24)). Obviously, both conclusions are not possible. However, this is the expected result for $\bar{R}^{2100}_{2025}$ and $\bar{R}^{2064}_{2062}$ if charge exchange is the predominate pumping mechanism for the $4d^2D_{5/2}$ level while electron collisions are responsible for populating all other levels. In this case, Equation (18) would apply for $\bar{R}^{2100}_{2025}$ with $\sigma_{05} = \sigma_{07} = \sigma_{08} = 0$. But equations of the same T_e dependence as Equation (24) would apply for $\bar{R}^{2064}_{2062}$, $\bar{R}^{2502}_{2062}$, and $\bar{R}^{2558}_{2025}$. The results for $\bar{R}^{2502}_{2062}$ and $\bar{R}^{2558}_{2025}$ when $P_i > 280$ watts (Fig. 3) do not show a clear increase or decrease with T_e. Since both the 2502 and 2558 Å transitions originate from the $5s^2S_{1/2}$ level, the T_e dependence of $\bar{R}^{2502}_{2062}$ and $\bar{R}^{2558}_{2025}$ must be the same. Therefore, the data of Figure 3 are more an indication of the experimental error than a clear indication that $\bar{R}^{2502}_{2062}$ and $\bar{R}^{2558}_{2025}$ are increasing or decreasing functions of T_e.

Data in Figure 4 also indicate that charge transfer is populating the $4d^2D_{5/2}$ level while electron collisions are responsible for the population of all other levels. The intensity ratio $\bar{R}^{2100}_{2558}$ shows a definite decrease with increasing T_e for $P_i > 280$ watts as expected (see

Eq. (26)). There is no clear indication that $\bar{R}^{2064}_{2558}$ is either an increasing or decreasing function of T_e. Within the experimental error, $\bar{R}^{2064}_{2558}$ would appear to be independent of T_e. As discussed earlier (see Eq. (22)), $\bar{R}^{2064}_{2558}$ would appear independent of T_e for charge exchange pumping of the 4d and 5p levels. However, when charge exchange is negligible (see Eq. (25)) it is not possible to conclude if $\bar{R}^{2064}_{2558}$ should increase or decrease with T_e.

Zn-Ar Results

Further evidence for charge exchange pumping of the $4d^2D_{5/2}$ level is obtained by comparing results in Zn-Ar with the Zn-Ne results. In Zn-Ar electron pumping is the only likely mechanism for populating the 4d and 5p levels and $\bar{R}^{2100}_{2558}$ will be given by Equation (25) and a similar expression for $\bar{R}^{2064}_{2558}$. It is possible that charge exchange to to the 4p levels of Zn^+ may occur ($\Delta E = 0.355$ eV), however, this will not effect $\bar{R}^{2100}_{2558}$ and $\bar{R}^{2064}_{2558}$.

The results for $\bar{R}^{2100}_{2558}$ and $\bar{R}^{2064}_{2558}$ in Zn-Ar are shown in Figure 5 together with T_e results in pure Ar. The electron temperatures in Ar are lower than in Ne and show the same erratic behavior for low input powers. The intensity ratios show rather inconsistent behavior also. As pointed out in the discussion following Equation (25) it is not possible to predict the electron temperature dependence of $(R^{2100}_{2558})_e$ and $(R^{2064}_{2558})_e$.

It is of interest to compare the magnitude of R^{2100}_{2558} and R^{2064}_{2558} in Zn-Ar with the Zn-Ne results. The ratio of $\langle R^{2100}_{2558} \rangle$ for Zn-Ne to $\langle R^{2100}_{2558} \rangle$ for Zn-Ar is 1.26. The ratio of $\langle R^{2064}_{2558} \rangle$ for Zn-Ne to $\langle R^{2064}_{2558} \rangle$ for Zn-Ar is 0.75. Note that it is the average measured intensity ratios that are being compared, not the normalized intensity ratios shown in Figures 4 and 5. The average value in Zn-Ne was computed using the data points for $285 \leq P_i \leq 520$ watts. In Zn-Ar the average value was computed using the data for $250 \leq P_i \leq 320$ watts. These are the power ranges where T_e is an increasing function of power input, P_i.

If electron collisions are populating the $4d^2D_{3/2}$ and $4d^2D_{5/2}$ levels in both Zn-Ne and Zn-Ar then the ratios should be nearly equal. However, the R^{2100}_{2558} ratio is nearly twice the R^{2064}_{2558} ratio. Since electron collisional pumping cannot produce such a result, it is concluded that charge transfer must be responsible for pumping the $4d^2D_{5/2}$ level in Zn-Ne.

Charge Exchange Cross-Section Limit

Collins[1] measured the total charge exchange cross-section for He^+ on Zn. He gives a value of 2.3×10^{-15} cm^2. The results of this experiment indicate a much larger cross section for the $4d^2D_{5/2}$ level than the

$4d^2D_{3/2}$ level. A lower limit on how much larger the $4d^2D_{5/2}$ cross section, σ_{06}, is than the $4d^2D_{3/2}$ cross section, σ_{05}, can be obtained from the data.

Using Equations (3) and (4) for the $4d^2D_{3/2}$ (i = 5) and $4d^2D_{5/2}$ (i = 6) levels together with Equation (17c) and

$$W_5 = n_e \sum_{i=1}^{4} n_i S_{i5} + n_o n_{Ne^+} U\sigma_{05} \tag{29}$$

the following is obtained:

$$R_{2064}^{2100} = \frac{2064}{2100} \frac{A_{52} + A_{53}}{A_{53}} \frac{\frac{\sigma_{06}}{\sigma_{05}}}{F(T_e) + 1} \tag{30}$$

where

$$F(T_e) = \left(\frac{n_e}{n_o n_{Ne^+}} \sum_{i=1}^{4} n_i S_{i5} \right) \frac{1}{U\sigma_{05}} \tag{31}$$

The measured intensity ratio, $(R_{2064}^{2100})_m$, in Zn-Ne was found to be approximately 1.9. Therefore, using Equation (30):

$$\frac{\sigma_{06}}{\sigma_{05}} = 1.9 \frac{T_{2064}}{T_{2100}} \frac{A_{52} + A_{53}}{A_{53}} [F(T_e) + 1] \tag{32}$$

The function $F(T_e)$ is the ratio of electron collisional pumping to charge exchange pumping of the $4d^2D_{3/2}$ level. As already discussed, the experimental results show that electron pumping predominates over charge exchange pumping of the $4d^2D_{3/2}$ level. Therefore, $F(T_e) > 0$. Using the transition probability data in Figure 1 and the estimated transmission ratio $T_{2064}/T_{2100} \approx 0.8$ the following lower limit is obtained.

$$\frac{\sigma_{06}}{\sigma_{05}} > 1.8 \tag{33}$$

The energy difference between the $4d^2D_{3/2}$ and $4d^2D_{5/2}$ levels is small (~0.006 eV). Therefore, it was expected that each of the states of the J = 3/2 and J = 5/2 levels to have the same probability of being populated by charge exchange. As a result, it is expected that the cross section ratio, σ_{06}/σ_{05}, should equal the ratio of statistical weights, 3/2. However, the experimental results indicate a lower limit of 1.8. In the case of Ca-Xe (Ref. 2) for charge exchange to the $4d^2D_{5/2}$ and

$4d^2D_{3/2}$ levels of Ca^+, it was found that the ratio of cross sections was ~1.13, which is close to the statistical weight ratio 3/2. However, for Ca^+ the energy difference between $4d^2D_{3/2}$ and $4d^2D_{5/2}$ is less than 0.003 eV. Turner-Smith[7] et al. investigating Zn-He found for the $6p^2P_{3/2}$ and $6p^2P_{1/2}$ levels (energy difference = 0.009 eV) a charge exchange cross section ratio of 7.5 compared to a statistical weight ratio of 2. For the $5d^2D_{5/2}$ and $5d^2D_{3/2}$ levels the energy difference is only 0.003 eV and the experimental result[7] for the cross section ratio is 1.8. This agrees fairly well with the statistical weight ratio of 1.5.

Melius[8] has presented arguments as to why two nearly resonant atomic states, such as $4d^2D_{5/2}$ and $4d^2D_{3/2}$ could have substantially different charge exchange cross sections. As Melius shows, the important region for charge transfer occurs at large internuclear separations. At these large distances the Ne^+ ($^2P_{3/2}$, $^2P_{1/2}$) ion and the Zn atom have not yet interacted. Thus the various molecular potential curves which can be obtained by combining Ne^+-Zn will remain essentially flat.

For Ne (^1S_o) combining with Zn^+ ($4d^2D_{5/2}$, $4d^2D_{3/2}$) five molecular states can be formed, three of them ($\Sigma_{1/2}$, $\pi_{3/2}$, $\Delta_{5/2}$) correlating with $4d_{5/2}$ and two of them ($\pi_{1/2}$, $\Delta_{3/2}$) correlating with $4d^2D_{3/2}$. The $\Sigma_{1/2}$ state will be repulsive (due to Pauli exclusion) at much larger values of internuclear separation than the remaining molecular states. Because of the slightly positive value of energy defect, the $\Sigma_{1/2}$ state will have its molecular potential energy curve cross those of the incident Ne^+-Zn system at a large value of separation giving rise to a large cross section. As Melius[8] discusses, if the $4d^2D_{5/2}$, $4d^2D_{3/2}$ splitting is too large, a fine structure transition from the 5/2 to the 3/2 state will be impeded and the outgoing system will preferentially remain in the $4d^2D_{5/2}$ state.

For Zn-Ne^+ charge transfer to the 5p levels of Zn^+, the energy defect is less than zero ($\Delta E < 0$). Therefore, the potential energy curves for $Ne^+(^2P_{3/2}, ^2P_{1/2})$ - $Zn(^1S_o)$ and $Ne(^1S_o)$ - $Zn^+(5p^2P_{1/2}, 5p^2P_{3/2})$ will not intersect. If the charge transfer process can be described by curve crossings of molecular states formed during the collision, then for $\Delta E < 0$, no charge exchange is expected to occur.[8] No experimental evidence of charge exchange to the 5p levels was obtained. This implies that the curve crossing model is applicable in the Zn-Ne system.

CONCLUSION

Experimental evidence indicates that charge exchange between Ne^+ and Zn is the dominate pumping mechanism of the $Zn^+(4d^2D_{5/2})$ level. The intensity ratios $\frac{\bar{R}2100}{2025}$ and $\frac{\bar{R}2100}{2558}$, which are proportional to the ratio of the $4d^2D_{5/2}$ to $4p^2P_{3/2}$ level and $4d^2D_{5/2}$ to $5s^2S_{1/2}$ level number densities, are decreasing functions of the electron temperature. This is the expected result if charge exchange is responsible for populating the $4d^2D_{5/2}$ level. A comparison between Zn-Ar and Zn-Ne data also indicates charge exchange pumping of the $4d^2D_{5/2}$ level. In Zn-Ar only electron

collisions can populate the 4d and 5s levels. It was found that the ratio $\langle R^{2100}_{2558} \rangle$ Zn-Ne$/\langle R^{2100}_{2558} \rangle$ Zn-Ar was nearly twice the ratio $\langle R^{2064}_{2558} \rangle$ Zn-Ne$/\langle R^{2064}_{2558} \rangle$ Zn-Ar. If electron collisional pumping is populating both the $4d^2D_{3/2}$ and $4d^2D_{5/2}$ levels in Zn-Ne then these two ratios should be nearly equal. Since this is not the case, it is concluded that charge transfer must be responsible for pumping the $4d^2D_{5/2}$ level. There is no evidence to indicate that charge exchange is the dominate pumping mechanism for the $4d^2D_{3/2}$, $5p^2P_{1/2}$, or $5p^2P_{3/2}$ levels, which also have small energy defects, ΔE.

A lower limit of 1.8 was obtained for the charge exchange cross section ratio, σ_{06}/σ_{05}, where σ_{06} is the cross section for the $4d^2D_{5/2}$ level and σ_{05} is the cross section for the $4d^2D_{3/2}$ level.

REFERENCES

1. G. J. Collins, J. Appl. Phys. 42, 3812 (1971).

2. D. L. Chubb, J. Appl. Phys. 46, 362 (1975).

3. D. R. Bates and A. Damgaard, Phil. Trans. R. Soc. (London), A242, 101 (1949).

4. G. J. Collins, unpublished.

5. R. C. Elton, "Methods of Experimental Physics, Plasma Physics," vol. 9A, edited by H. R. Griem and R. H. Lonberg (Academic, New York, 1970), p. 115.

6. P. O. Taylor and G. H. Dunn, Phys. Rev. A8, 2304 (1973).

7. A. R. Turner-Smith, J. M. Green, and C. W. Webb, J. Phys. B, 6, 114 (1973).

8. C. F. Melius, J. Phys. B, 7, 1692 (1974).

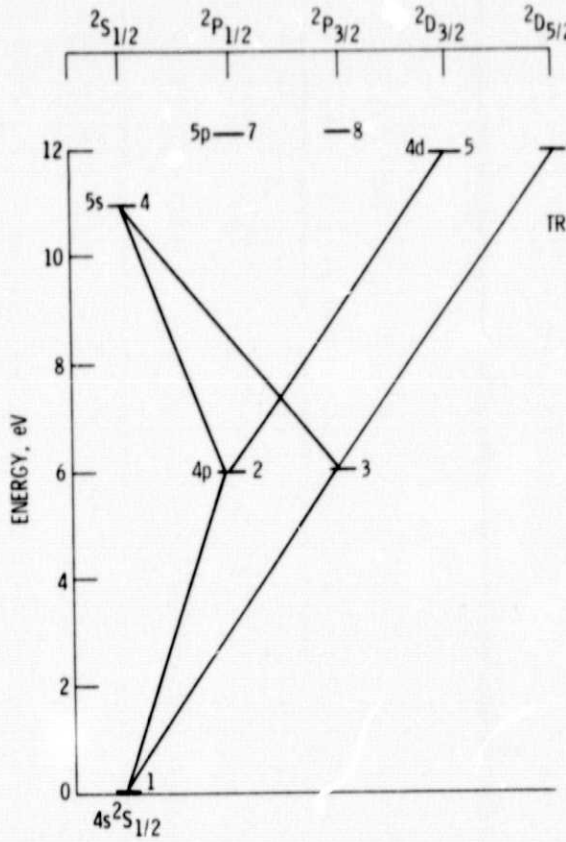

TRANSITION, i → j	TRANSITION PROBABILITY, A_{ij}, SEC^{-1}	WAVELENGTH, λ_{ij}, Å
2 → 1	$4.56 \times 10^{+8}$	2 062
3 → 1	4.82	2 025
4 → 2	1.31	2 502
4 → 3	2.59	2 558
5 → 2	6.43	2 064
5 → 3	1.26	2 102
6 → 3	7.54	2 100
7 → 4	.505	7 733
7 → 5	.105	22 440
7 → 1	.059	987
8 → 4	.531	7 589
8 → 5	.022	21 268
8 → 6	.130	21 500
8 → 1	.091	984

Figure 1. - Energy level diagram for zinc ion.

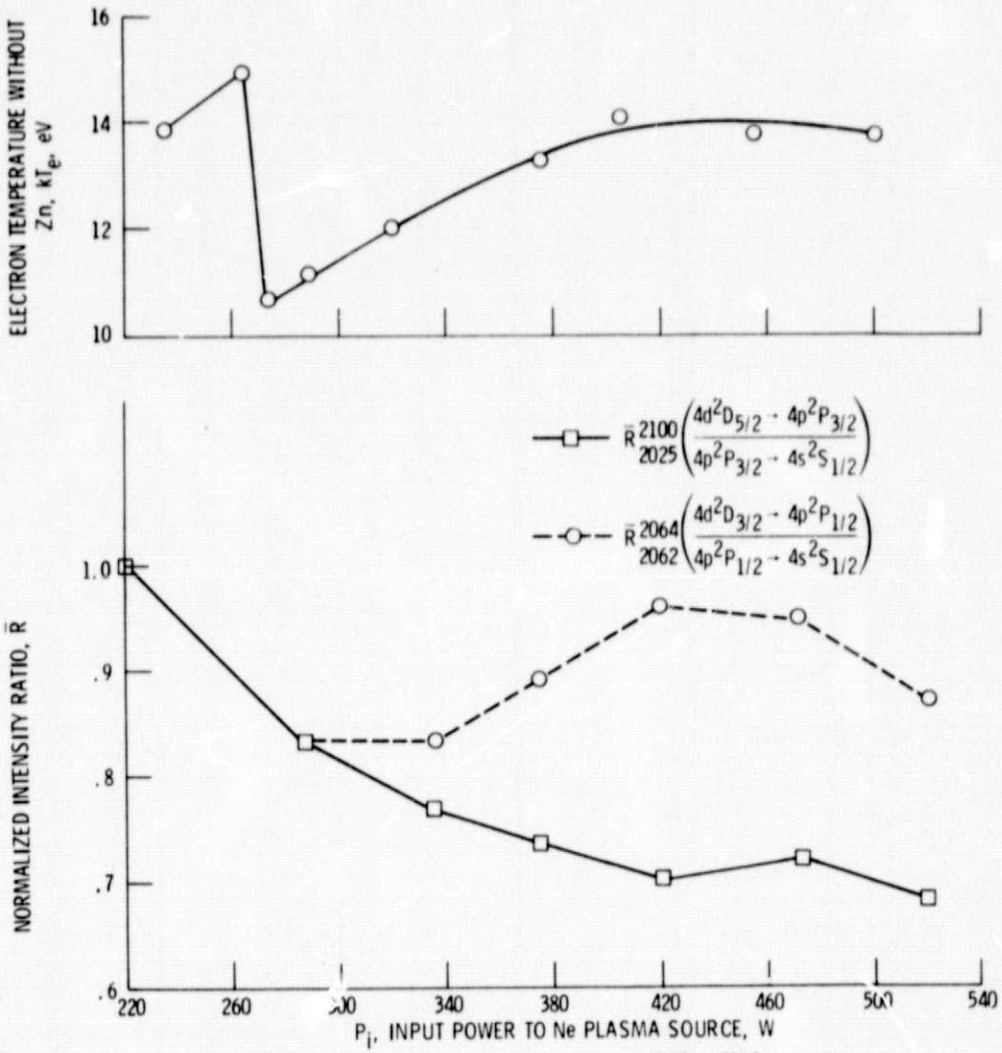

Figure 2. - Electron temperature and intensity ratios $\bar{R}\frac{2100}{2025}$, $\bar{R}\frac{2064}{2062}$ versus power input in Zn-Ne.

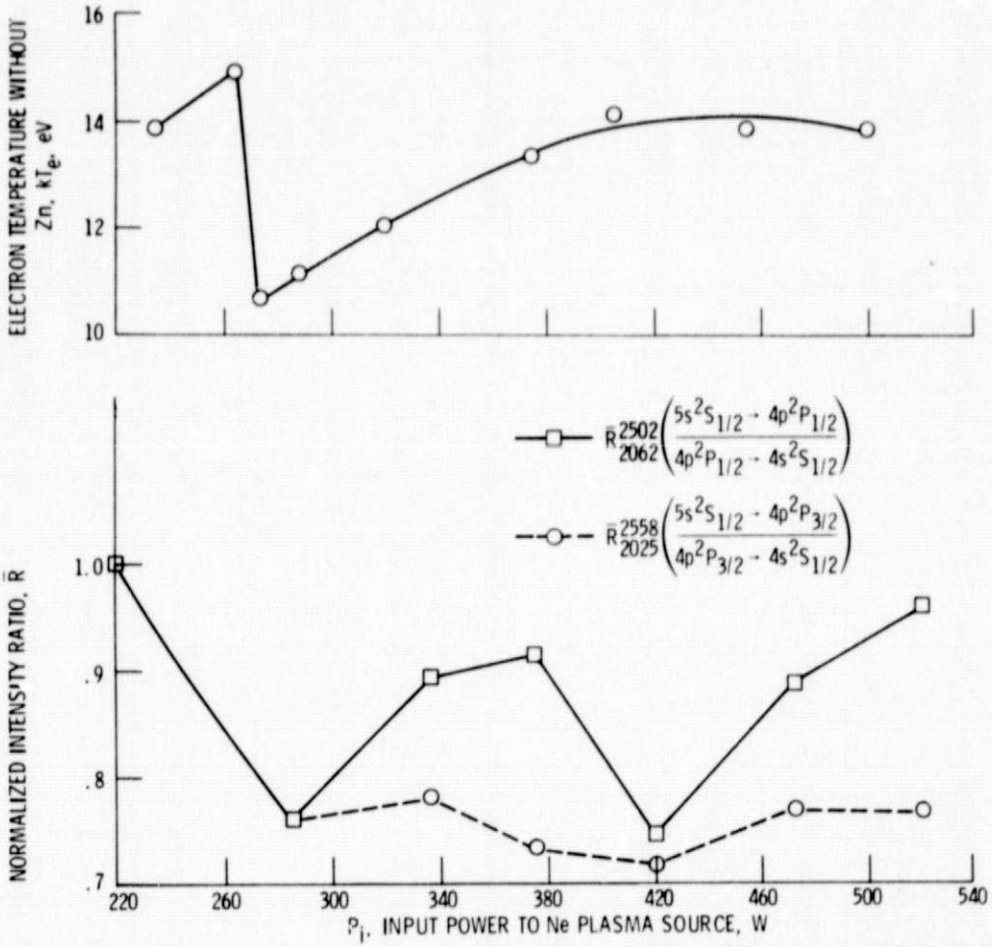

Figure 3. - Electron temperature and intensity ratios $\bar{R}^{2502}_{2062}$, $\bar{R}^{2558}_{2025}$ versus power input in Zn-Ne.

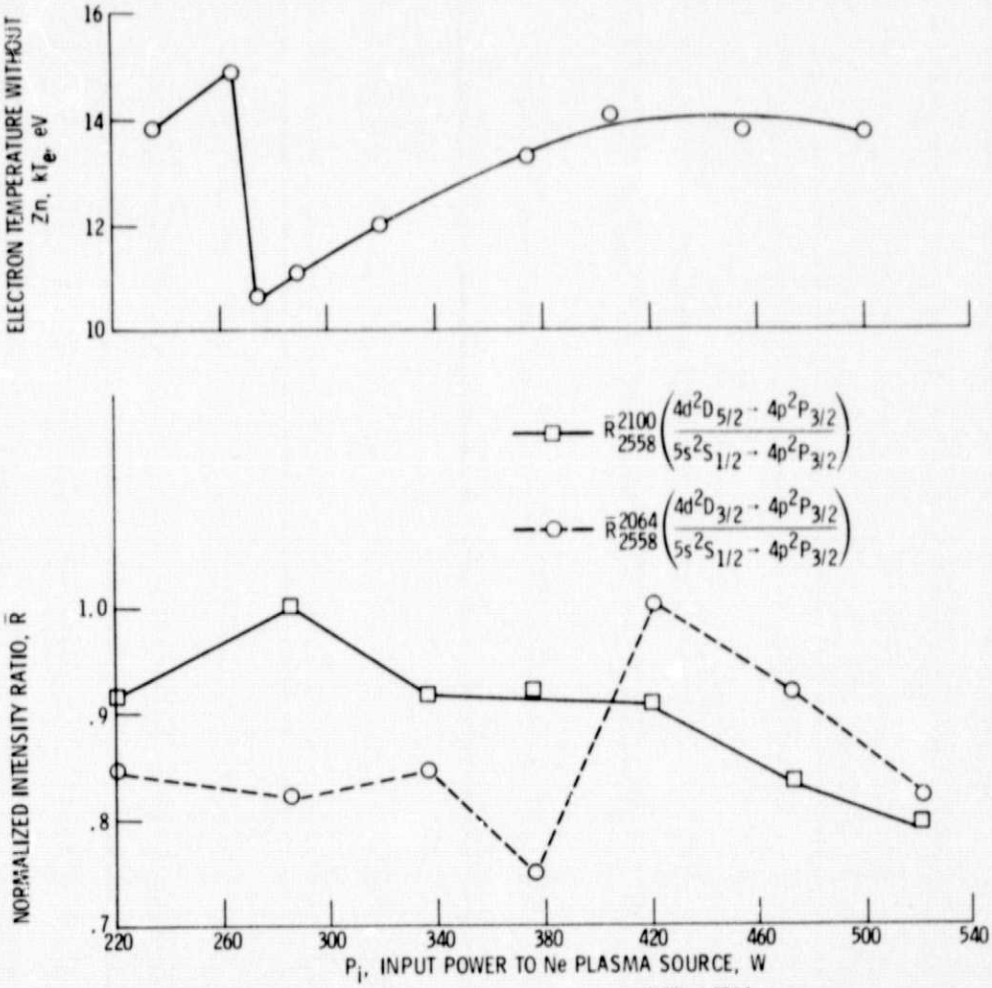

Figure 4. - Electron temperature and intensity ratios $\bar{R}^{2100}_{2558}$, $\bar{R}^{2064}_{2558}$ versus power input in Zn-Ne.

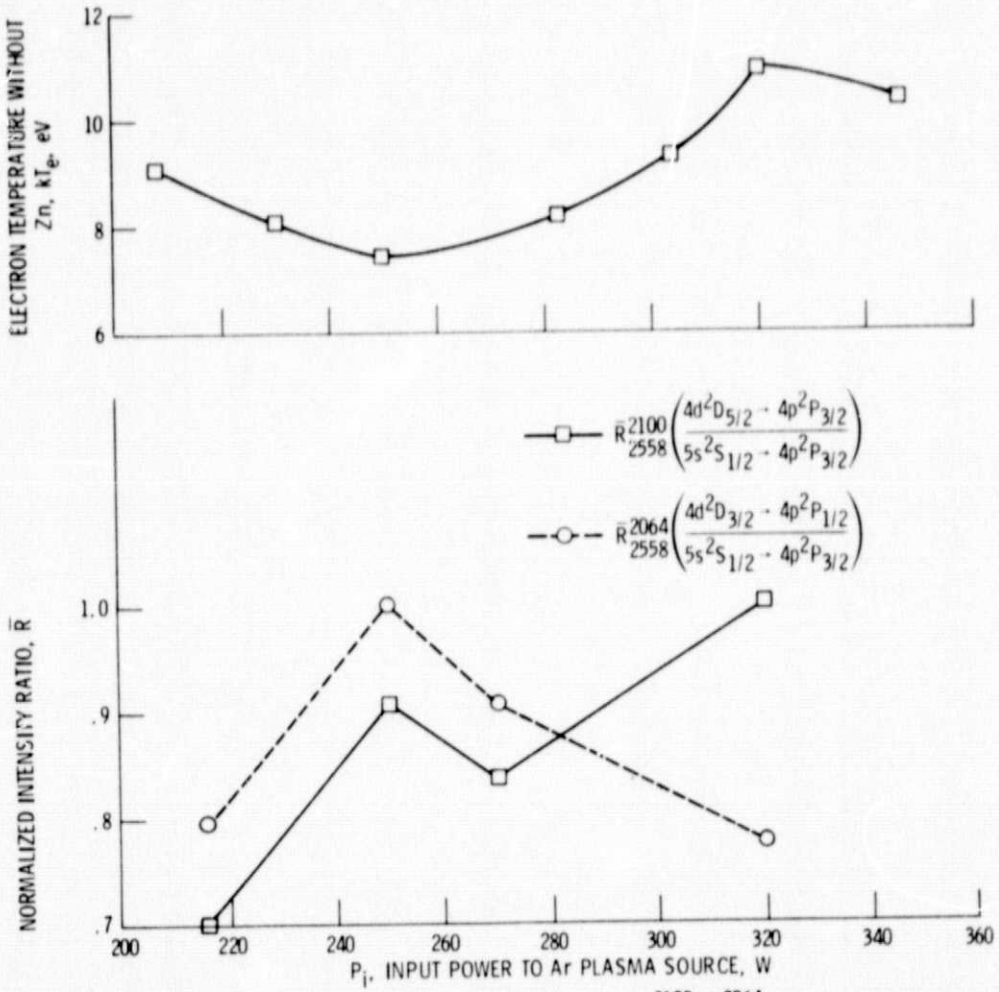

Figure 5. - Electron temperature and intensity ratios $\bar{R}^{2100}_{2558}$, $\bar{R}^{2064}_{2558}$ versus power input in Zn-Ar.